

Synthesis of thin-walled carbon nanotubes from methane by changing the Ni/Mo ratio in a Ni/Mo/MgO catalyst

ZHANG Qiang, LIU Yi, HU Ling, QIAN Wei-zhong*, LUO Guo-hua, WEI Fei*

Beijing Key Laboratory of Green Reaction Engineering and Technology, Department of Chemical Engineering, Tsinghua University, Beijing 100084, China

Abstract: Thin-walled carbon nanotubes (CNTs) were prepared from methane decomposition using Ni/Mo/MgO as catalysts loaded with 1% mole fraction of Ni and smaller proportion of Mo. The relationship between CNT diameter and Ni/Mo ratio was studied by SEM, TEM, XRD and Raman spectroscopy. The particle size and the active phase of the catalyst could be modulated by the Ni/Mo ratio. With decreasing Ni/Mo ratio, a NiMo alloy was first formed, and then an isolated Mo phase was formed on the catalyst, as characterized by TEM and XRD. The NiMo alloy, with very small size, was responsible for the growth of thin-walled CNTs, whereas, the Mo phase was related to the formation of large-diameter thick-walled CNTs. The thin-walled CNTs with outer diameter of 3.0 nm and inner diameter of 1.3 nm could be obtained with high selectivity, a narrow diameter distribution, and high purity by controlling the Ni/Mo ratio at 6. Raman spectra confirmed the formation of thin-walled CNTs with few defects. The formation of thin-walled CNTs was mainly attributed to a rapid surface diffusion and precipitation of carbon on the small metal alloy crystallites.

Key Words: Carbon Nanotubes; Chemical vapor deposition; Ni/Mo/MgO

1 Introduction

Carbon nanotubes (CNTs), with excellent electrical and mechanical properties, have potential applications in conductive and high-strength composite, sensor, field emission display, hydrogen storage, nanoscale devices etc^[1–5]. Among those applications, the reinforced effect of CNTs in polymer or ceramic material composites has been the most attractive one, owing to a very large market for these functional materials. It has been proved that single walled CNTs (SWCNTs) have good performance in super-reinforced composite materials^[5]. However, due to difficulty in synthesis of SWCNTs in large scale and at low cost, it has not been possible to achieve exciting results in this area. Fortunately, Branimir Lukic recently reported the similar high mechanical strength of thin multi-walled CNTs to that of SWCNTs^[6], offering possibilities to achieve an excellent reinforced effect by CNTs. Another research showed that the smaller the diameter of the CNTs, the better the field emission due to their large field enhancement factor^[7]. These results will stimulate a controlled synthesis of thin-walled and small diameter CNTs.

To synthesize thin-walled and small diameter CNTs, catalyst should be prepared having very small crystallites, sintering of which should be inhibited during growth of CNTs. Metals supported on inorganic materials including Al₂O₃, SiO₂ or MgO etc have always been used as catalysts, owing to an effective dispersion of metal crystallites in nanometer scale on

supports. For example, thin-walled CNTs can be achieved by using Co–Mo, Co–V, and Co–Fe catalysts supported either on zeolite or corundum alumina or by Fe/Mo/MgO catalyst^[8]. As recently reported, 2–5-walled CNTs with high purities (over 90%) were prepared from CH₄ over Mo/Ni/MgO catalysts at 1073 K^[9].

These successful examples confirmed the effectiveness of bimetallic catalyst in the synthesis of thin-walled CNTs, such as Fe/Mo^[10], Ni/Mo^[9,11,12], Co/Mo^[13], Fe/Co^[14] catalysts. For the potential catalytic action of Ni/Mo/MgO for thin-walled CNTs synthesis^[9], Li et al^[11] prepared Ni/Mo/MgO catalyst with combustion method, which has a 8000% yield of per gram catalyst for multi-walled CNTs. Shimizu et al^[12] obtained cone-shaped CNT assemblies with Ni/Mo catalyst sputtered on a silicon wafer. However, the loading of metals on supports is still high (i.e. 5% mole fraction of Ni/Mo loading in previous study)^[6–12]. It might be too high and was unfavorable for the effective dispersion of metal crystallites on the support. Some other operating conditions, such as reaction atmosphere and carbon source in the controllable synthesis of CNTs, were also discussed by several authors^[15–19]. To achieve a more precise control on the wall number and diameter of the as-grown CNTs, the authors further decreased the loading of Ni and Mo species to about 1–1.5% mole fraction for Ni/Mo/MgO catalyst. It was expected that good dispersion effect could be achieved. And the detailed investigations using TEM, SEM, XRD, and Raman

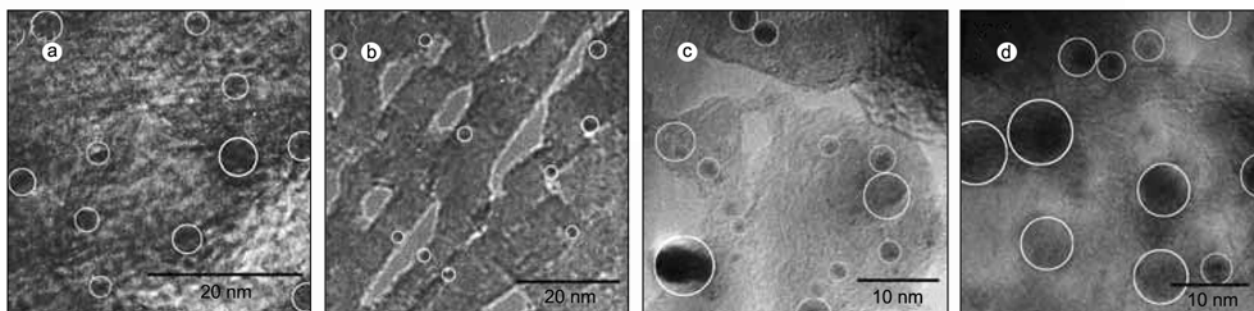


Fig.1 TEM images of catalysts after reduction and with 10s contact with carbon sources (fixed Ni mole fraction at 0.01, a Ni/Mo=1:0; b Ni/Mo=6:1; c Ni/Mo=1:1; d Ni/Mo=1:4)

spectroscopy confirmed the effectiveness of tailoring the Ni/Mo loading and the Ni/Mo ratio of the catalyst to control the morphology of CNTs. On the other hand, the authors also found complex states of Ni and Mo species as a result of a small Ni/Mo loading and a relatively wide Ni/Mo ratio. The formation mechanism of such thin-walled CNTs from the small size nanocrystallite catalysts is discussed based on these findings.

2 Experimental

2.1 Catalyst preparation

The Ni/Mo/MgO catalyst was prepared by a coprecipitation method. During the catalyst preparation process, the solution of $\text{Mg}(\text{NO}_3)_2 \cdot 6\text{H}_2\text{O}$ and $\text{Ni}(\text{NO}_3)_2 \cdot 6\text{H}_2\text{O}$ was precipitated from a basic solution containing $(\text{NH}_4)_2\text{CO}_3$ and molybdenum ions at 293–353 K. After filtration, and drying at 383 K for 20 h and calcination at 673 K for 5 h, the catalyst consisted of nickel and molybdenum oxides supported over magnesia. Finally, faintly green materials were obtained, which were ground to fine powders. Further details of the preparation of the catalyst can be found elsewhere^[20].

2.2 CNT synthesis

To synthesize multiwalled CNTs (MWCNTs), approximately 100 mg of the catalyst was sprayed uniformly into a quartz boat, which was inserted in the center of a quartz tube (id: 25 mm, length: 1 200 mm). The quartz tube, mounted in an electrical tube furnace, was heated to 600 °C, in an air atmosphere. Subsequently, argon was fed at a flow rate of 600 mL/min. And the H_2 flew into the reactor at 600 °C at a rate of 50 mL/min for 30 min for low temperature reduction of catalyst. High temperature catalyst reduction was carried out at 900 °C. After reduction, the reactor was heated to reaction temperature and a mixture of CH_4/H_2 (100/50 mL/min, V/V) was introduced into the quartz tube and maintained at the reaction temperature for 60 min before the furnace was cooled to room temperature under Ar protection.

2.3 Characterization

The morphology of the CNTs was characterized by high resolution scanning electron microscopy (JSM 7401F at 5.0

kV) high resolution transmission electron microscopy (JEM 2010 at 200.0 kV). Raman spectra experiments were performed with a Raman spectrophotometer Renishaw, RM2000 in ambient condition. The spectra were recorded using a He-Ne laser excitation line 633.0 nm. Powder X-ray diffraction (XRD) patterns of the catalysts were obtained with an O8DISCOVER diffractometer by use of nickel-filtered Cu K α radiation. The patterns were recorded between 10° and 90°.

3 Results and discussion

3.1 Characterization of catalyst

3.1.1. TEM observation of catalyst

The authors characterized Ni/Mo/MgO catalysts with a fixed Ni mole fraction of 0.01 by TEM in order to reveal the catalyst particles on the carrier. Fig.1 shows typical TEM images of reduced catalysts with 10s contacting with carbon sources. The authors always observed dark spherical particles distributed on bright cubic crystals, where the number of the dark spheres increased with increasing Mo fraction. It is well known that MgO phase have a cubic structure. The dark and bright particles were thus attributed to metal particles consisting of Ni and/or Mo and to MgO crystals, respectively. For the Ni/MgO catalyst, nickel particle covered MgO surface in a high density (Fig.1a), whereas, in the Ni/Mo/MgO catalyst with a Ni/Mo ratio of 6, much smaller catalyst particle deposited on the edge of the MgO crystal. And for the Ni/Mo/MgO with the Ni/Mo ratio of 1 and 0.25, the catalyst particles dispersed on the MgO surface were with an obvious contrast.

The catalyst particles on the carriers showed various sizes and the authors examined the distribution of metal nanoparticles by measuring the sizes and counting these particles in the TEM images. From the particle size distribution for the reduced catalyst, it can be seen that the size of reduced metal catalyst (Fig.1b–d) became larger and the distribution became broader with increasing Mo ratio. However, small amount of Mo could reduce the size of metal catalyst compared with Ni/MgO catalyst (Fig.1a).

3.1.2 XRD of catalyst

The bulk crystal structures of catalysts and their sizes before and after the catalyst reduction were then examined by

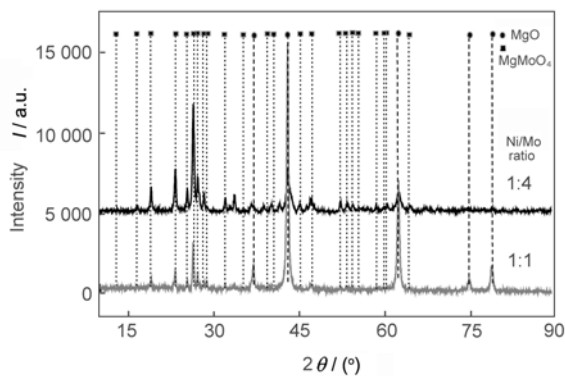


Fig.2 XRD patterns of catalysts before reduction at 923 K for 0.5 h (fixed Ni mole fraction at 0.01)

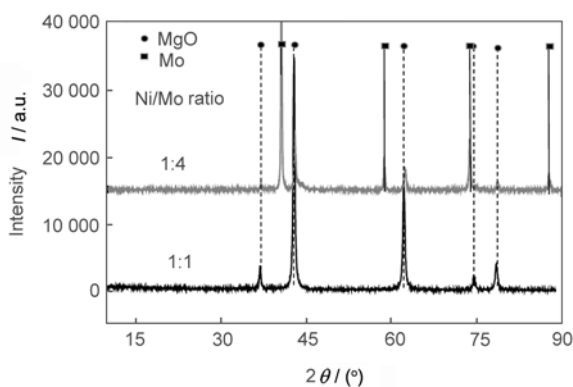


Fig.3 XRD patterns of catalysts after reduction at 923 K for 0.5 h (fixed Ni mole fraction at 0.01)

XRD. The Ni/Mo/MgO catalysts mainly contain MgO and MgMoO₄ phase as shown in Fig.2. With more Mo mole fraction, the peak of MgMoO₄ phase was higher. According to Scherrer formulation, the size of MgMoO₄ phase was 30 nm for the catalyst with Ni/Mo ratio of 0.25, and was 44 nm for the catalyst with Ni/Mo ratio of 1. NiO was mainly nanoparticles on the carrier surface, so it was difficult to obtain an obvious diffraction peak in the XRD pattern. After the catalyst reduction, the peak of MgMoO₄ phase disappeared. For the catalyst with Ni/Mo ratio of 0.25, the peak intensity of Mo phase was increased (Fig.3). Meanwhile, its size was about 39

nm, smaller than the size of MgMoO₄ phase before catalyst reduction. There were enough Mo particles dispersed on the reduced catalyst. When the catalyst of Ni/Mo ratio was 1, the Ni and Mo particles were too small to show their diffraction peaks in agreement with the TEM results. According to other reports, Ni and Mo formed alloys and Mo can seclude Ni particles which can prevent Ni nanoparticles from congregating under high temperature^[9,13]. With more fraction of Mo, Ni and Mo can form alloys first, then more Mo atoms will form an isolated Mo phase on the reduced Ni/Mo/MgO catalyst, which will be discussed in detail later.

3.2 Morphology and structure of CNTs

Catalysts with fixed Ni of 1% mole fraction and different Ni/Mo ratios were prepared to study the effect of Ni/Mo ratio on CNT growth. The morphology of CNTs synthesized from methane at 1 273 K for 1 h can be seen in Figs.4 and 5. Large amount of CNTs were grown from catalyst particles and the CNTs wrapped the catalysts. Agglomerate CNTs were obtained, which were different from the morphology of CNTs bundles shown in Ref. 11 or cone-shaped CNT assemblies shown in Ref. 12. The products were free of amorphous carbon, indicating high purity, although it was difficult to determine by SEM or TEM quantitatively. The purity of CNTs was always higher for the carbon product synthesized with longer reaction time of 3 h than for that synthesized for 1 h, suggesting that the impurities may not be carbonaceous but may be due to the catalysts used for the CNT synthesis. TEM results (Fig.5) showed that thin-walled CNTs were produced for all the catalyst used.

Except Fig.4d of SEM results, the as-grown CNTs had nearly uniform diameter. Two kinds of CNTs with obvious different diameters were obtained and the arrows pointed to large diameter CNTs. TEM observations (Fig.5) confirmed this point. The authors thus analyzed the dependence of thickness and diameter of CNTs on the catalyst composition for the Ni/Mo/MgO catalyst series with fixed Ni contents. It can be seen that adding small amount of Ni was effective to decrease the diameters and the number of graphene layers compared with Fig.1a and 1b. And the inner diameters, the outer diameters and the numbers of layers of the CNTs increased with increasing Mo mole fraction. At the lower Mo

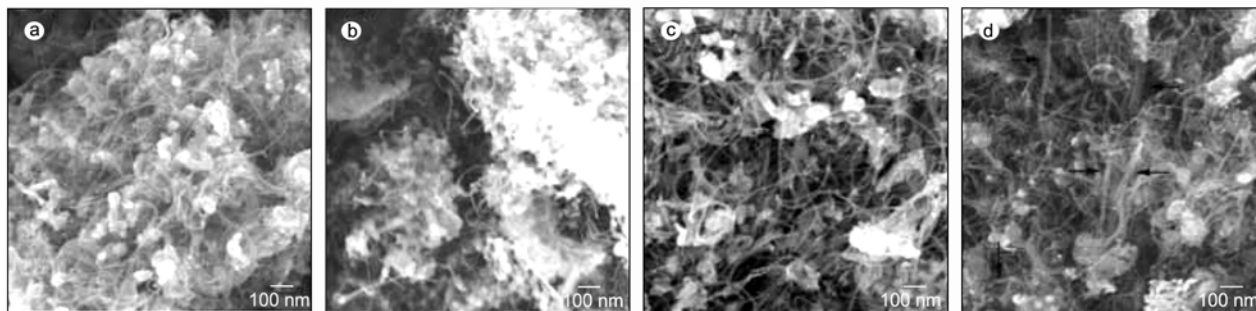


Fig.4 SEM images of the as-grown CNTs produced by catalytic decomposition of CH₄ at 1273 K for 1 h over Ni/Mo/MgO catalysts (fixed Ni mole fraction at 0.01, a Ni/Mo = 1:0; b Ni/Mo = 6:1; c Ni/Mo = 1:1; d Ni/Mo = 1:4)

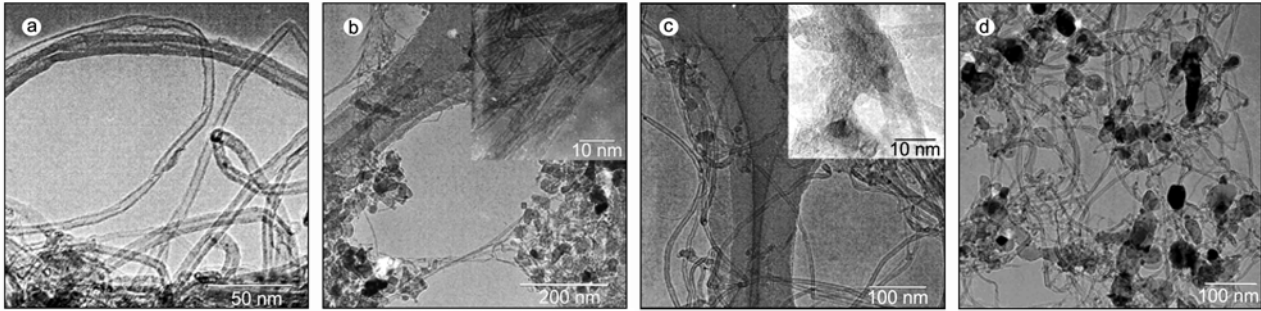


Fig.5 TEM images of the as-grown CNTs produced by catalytic decomposition of CH₄ at 1273 K for 1 h over Ni/Mo/MgO catalysts (fixed Ni mole fraction at 0.01, a Ni/Mo = 1:0; b Ni/Mo = 6:1; c Ni/Mo = 1:1; d Ni/Mo = 1:4)

mole fraction of 0.017, the inner and outer diameters ranged from 1.0 to 3.0 nm and from 2.5 to 5.0 nm, respectively. At the higher Mo mole fractions, the distributions of the diameters as well as the thickness became broad. With a higher of Mo mole fraction of 4%, two kinds of CNTs were shown: one with the inner and outer diameters ranged from 2.0 to 4.0 nm and from 6.5 to 9.5 nm, respectively, and another one with the inner and outer diameters ranged from 6.0 to 11.0 nm and from 18.0 to 23.5 nm, respectively, which showed a broad diameter distribution of CNTs. The variation in the diameter was ascribed to the catalyst particle size and bimetallic catalyst ratio. Here, 2-5-walled CNTs have been selectively produced (more than 90%) by the decomposition of CH₄ over the Ni/Mo/MgO catalyst with Ni/Mo mole ratio of 6. That is, this catalyst is effective for the synthesis of thin-walled CNTs with narrow diameter distribution.

3.3 Raman Spectra of CNTs

Fig.6 shows the Raman spectra of the as-grown CNTs obtained over samples of Ni/Mo/MgO with a fixed Ni mole fraction of 0.01 at 1 273 K for 1 h. The results shown in Fig.6 indicate that the intensity of the G-band decreased, whereas, that of the D-band increased with increasing the Mo mole fraction from 0.017 to 0.040. The relationship between the I_G/I_D intensity ratio and the Mo mole fraction is also shown in Fig.6. The relative intensity of the G-band to the D-band decreased with increasing Mo mole fraction, indicating more defects in the as-synthesized CNTs. The CNTs products from catalyst adding Mo were with a higher I_G/I_D intensity ratio than Ni/MgO product, indicating that a better crystalline of CNTs was obtained. This was consistent with the TEM results mentioned above. This behavior has been observed for the CNT growth with Co/Mo/MgO catalysts by other authors^[13], which produced thick-walled CNTs at higher Mo fractions. When the Ni/Mo ratio was 6, the I_G/I_D intensity ratio of synthesized CNTs is 3.33, which was much higher than the ratio for the MWCNTs synthesized by nano-agglomerate fluidized bed (always at 1). This meant that high quality thin-walled CNTs were obtained from Ni/Mo/MgO catalyst with a Ni/Mo ratio at 6.

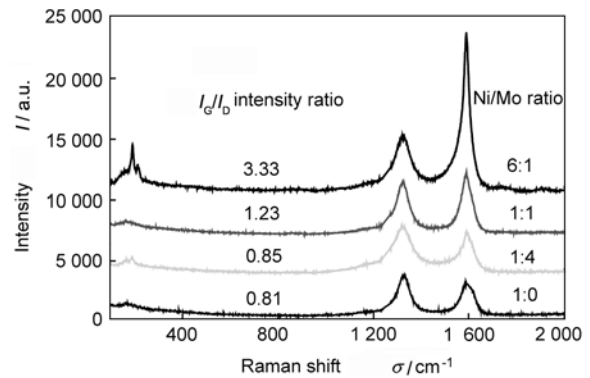


Fig.6 Raman spectra of CNTs synthesized over Ni/Mo/MgO catalysts (fixed Ni mole fraction at 0.01)

3.4 Proposed mechanism for modulating the diameter of CNTs

The authors analyzed TEM images of the CNTs and catalysts in order to examine the correlation between particle sizes of catalysts and CNT inner and outer diameters. When the ratio of Ni/Mo in the catalyst is 1:4, both the inner and outer diameter of CNTs and the reduced metal particle size show double peak distribution. By adding Mo, the inner diameter of CNTs agrees well with the reduced metal particle size, and a rapid surface diffusion play an important role in CNT growth. Also the change of variance shows the same tendency for the reduced metal particle size, and the inner and the outer diameter of CNTs. Thus, the diameter of CNTs depends on the size of metal nanoparticles on the support, in accord with the reports by the other authors^[21].

The diameter of CNTs was sensitive to the size of metal particle at the reaction condition. For Ni/MgO catalyst (Fig.7), although Ni could form small particles at first, the nickel nanoparticles were easy to congregate to form larger particles that form larger diameter CNTs. With little addition of Mo, Ni and Mo formed alloys and kept the size of active catalyst particles unchanged at high temperature. So narrow distribution of thin-walled CNTs were obtained at Ni/Mo ratio of 6 (Fig.7). With the Mo addition, some of the Mo atoms can agglomerate

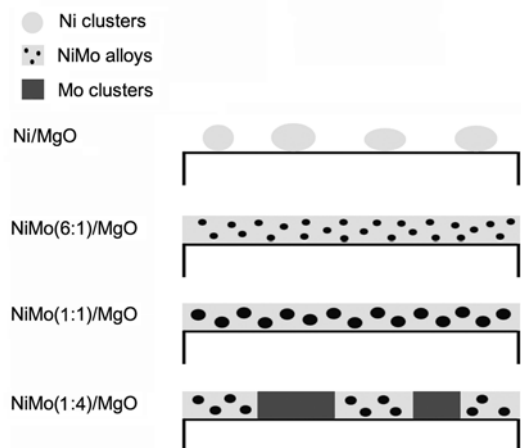


Fig.7 Schematic description of the structure of the different catalysts in the reduced state, as derived from the characterization methods

at the surface of NiMo alloy phase to provide small active catalyst particles, and another part will congregate together to form Mo particles. Mo particles also have activity to decompose methane to synthesize CNTs^[22]. So for the Ni/Mo/MgO catalyst with Ni/Mo ratio at 0.25, both the Ni/Mo alloy phase and Mo phase existed and double peak distribution of catalyst were formed and two kinds of CNTs with different diameters were produced during the synthesis process.

4 Conclusions

MWCNTs were produced by decomposition of CH₄ using Ni/Mo/MgO as catalysts in a controlled way with respect to the diameter and thickness of the CNTs. The average outer diameters and the numbers of layers were controlled from 3 to 23 nm and from 2 to 24, respectively, by changing the Mo fractions. With varying Mo loading on the catalyst support, Mo can form alloy with Ni and prevent Ni nanoparticles from segregating at high temperature. However, high fraction of Mo on the catalyst will form an isolated Mo phase in the reduced catalyst. So controlling the Ni/Mo ratio can affect active catalyst particle, and bimetallic nanoparticle sizes have great effect on the inner diameter of the CNTs. So the diameter of CNTs can be controlled by Ni/Mo ratio. The authors found that when the ratio of Ni/Mo is 6, 2-5 walled CNTs can be obtained with high selectivity and high purity, which provides an easy way to prepare thin-walled CNTs.

References

[1] Baughman R H, Zakhidov A A, de Heer W A. Carbon nanotubes - the route toward applications[J]. *Science*, 2002, **297** (5582): 787-792.
 [2] Dalton A B, Collins S, Munoz E, et al. Super-tough carbon-nanotube fibres - These extraordinary composite fibers can be woven into electronic textiles[J]. *Nature*, 2003, **423**(6941): 703.
 [3] Coleman J N, Khan U, Blau W J, et al. Small but strong: A re-

view of the mechanical properties of carbon nanotube-polymer composites[J]. *Carbon*, 2006, **44**(9): 1624-1652.
 [4] WU Feng, XU Bin. Progress on the application of carbon nanotubes in supercapacitors[J]. *New Carbon Materials*, 2006, **21**(2): 176-185.
 [5] WEI Fei, ZHANG Qiang, QIAN Wei-Zhong, et al. Progress on aligned carbon nanotube array[J]. *New Carbon Materials*, 2007, **22**(3): 271-282.
 [6] Lukic B, Seo J W, Bacsar R R, et al. Catalytically grown carbon nanotubes of small diameter have a high Young's modulus[J]. *Nano Letters*, 2005, **5**(10): 2074-2077.
 [7] de Jonge N, Allieux M, Doytcheva M, et al. Characterization of the field emission properties of individual thin carbon nanotubes[J]. *Applied Physics Letters*, 2004, **85**(9): 1607-1609.
 [8] Willems I, Konya Z, Colomer J F, et al. Control of the outer diameter of thin carbon nanotubes synthesized by catalytic decomposition of hydrocarbons[J]. *Chemical Physics Letters*, 2000, **317** (1-2): 71-76.
 [9] Zhou L P, Ohta K, Kuroda K, et al. Catalytic functions of Mo/Ni/MgO in the synthesis of thin carbon nanotubes[J]. *The Journal of Physical Chemistry Part B*, 2005, **109**(10): 4439-4447.
 [10] Qian W Z, Liu T, Wei F, et al. Carbon nanotubes containing iron and molybdenum particles as a catalyst for methane decomposition[J]. *Carbon*, 2003, **41**(4): 846-848.
 [11] Li Y, Zhang X B, Tao X Y, et al. Mass production of high-quality multi-walled carbon nanotube bundles on a Ni/Mo/MgO catalyst[J]. *Carbon*, 2005, **43**(2): 295-301.
 [12] Shimizu Y, Sasaki T, Kodaira T, et al. Fabrication of carbon nanotube assemblies on Ni-Mo substrates mimics law of natural forest growth[J]. *Chemical Physics Letters*, 2003, **370**(5-6): 774-780.
 [13] Herrera J E, Leandro B, Armando B, et al. Relationship between the structure/composition of Co-Mo catalysts and their ability to produce single-walled carbon nanotubes by CO disproportionation[J]. *Journal of Catalysis*, 2001, **204**(1): 129-145.
 [14] Coquay P, Flahaut E, De Grave E, et al. Fe/Co alloys for the catalytic chemical vapor deposition synthesis of single- and double-walled carbon nanotubes (CNTs). 2. The CNT-Fe/Co-MgAl₂O₄ system[J]. *The Journal of Physical Chemistry Part B*, 2005, **109**(38): 17825-17830.
 [15] WANG Mao-zhang, LI Feng, et al. Advances in synthesizing and preparing carbon nanotubes from different carbon sources[J]. *New Carbon Materials*, 2003, **18**(4): 250-264.
 [16] LI Ying, LI Xuan-ke, LIU Lang. The production of CNTs by catalytic decomposition of different source gases[J]. *New Carbon Materials*, 2004, **19**(4): 298-302.
 [17] LIU Yun-fang, SHEN Zeng-min, MA Bao-hai, et al. The effect of carbon source on the morphology of carbon nanotubes[J]. *New Carbon Materials*, 2003, **18**(4): 295-300.
 [18] LU Yi, ZHU Zhen-ping, LIU Zhen-yu. Effect of catalyst on the growth of carbon nanotubes using a detonation approach[J]. *New Carbon Materials*, 2004, **19**(1): 1-6.
 [19] ZHENG Rui-ting; CHENG Guo-an; ZHAO Yong; et al. Preparation and characterization of carbon nanoribbons produced by

- the catalytic chemical vapor deposition of acetylene[J]. *New Carbon Materials*, 2004, **20**(4): 355-359.
- [20] Qian W Z, Yu H, Wei F, et al. Synthesis of carbon nanotubes from liquefied petroleum gas containing sulfur[J]. *Carbon*, 2002, **40**(15): 2968-2970.
- [21] Cheung C L, Kurtz A, Park H K, et al. Delivery of catalytic metal species onto surfaces with dendrimer carriers for the synthesis of carbon nanotubes with narrow diameter distribution[J]. *The Journal of Physical Chemistry Part B*, 2002, **106**(48): 12361-12365.
- [22] Li Y, Zhang X B, Tao X Y, et al. Single phase MgMoO₄ as catalyst for the synthesis of bundled multi-wall carbon nanotubes by CVD[J]. *Carbon*, 2005, **43**(6): 1325-1328.